

Article

Comparison of Pedotransfer Functions for Determination of Saturated Hydraulic Conductivity for Highly Eroded Loess Soil

Agnieszka Petryk ^{1,*}, Edyta Kruk ², Marek Ryzek ² and Lenka Lackóová ³

- ¹ Department of Urban Management, Institute of Spatial Management and City Studies, College of Public Economy and Administration, Cracow University of Economics, Rakowicka 27 St, 31-510 Kraków, Poland
- ² Department of Land Reclamation and Environmental Development, Faculty of Environmental Engineering and Land Surveying, Agriculture University of Krakow, Mickiewicza 24/28 St, 30-059 Krakow, Poland
- ³ Institute of Landscape Engineering, Faculty of Horticulture and Landscape Engineering, Slovak University of Agriculture in Nitra, Hospodárska, 794901 Nitra, Slovakia
- * Correspondence: petryka@uek.krakow.pl; Tel.: +48-122-937-420

Abstract: Saturated hydraulic conductivity is one of the most essential soil parameters, influencing surface runoff and water erosion formation. Both field and laboratory methods of measurement of this property are time or cost-consuming. On the other hand, empirical methods are very easy, quick and costless. The aim of the work was to compare 15 pedotransfer models and determination of their usefulness for assessment of saturated hydraulic conductivity for highly eroded loess soil. The mean values obtained by use of the analyzed functions highly fluctuated between $2.00 \cdot 10^{-3}$ and $4.05 \cdot 10^0$ m·day⁻¹. The results of calculations were compared within them and with the values obtained by the field method. The function that was the best comparable with the field method were the ones proposed by Kazeny-Carman, based on void ratio and specific area, and by Zauerebrej, based on total porosity and effective diameter d_{20} . In turn, the functions that completely differed with the field method were the ones proposed by Seelheim, based on effective diameter d_{50} and by Furnival and Wilson, based on bulk density, organic matter, clay and silt content. The obtained results are very important for analysis among others water erosion on loess soil.



Citation: Petryk, A.; Kruk, E.; Ryzek, M.; Lackóová, L. Comparison of Pedotransfer Functions for Determination of Saturated Hydraulic Conductivity for Highly Eroded Loess Soil. *Land* **2023**, *12*, 610. <https://doi.org/10.3390/land12030610>

Academic Editor: Amrakh I. Mamedov

Received: 20 December 2022
Revised: 23 February 2023
Accepted: 24 February 2023
Published: 3 March 2023



Copyright: © 2023 by the authors. Licensee MDPI, Basel, Switzerland. This article is an open access article distributed under the terms and conditions of the Creative Commons Attribution (CC BY) license (<https://creativecommons.org/licenses/by/4.0/>).

Keywords: saturated hydraulic conductivity; pedotransfer functions; loess soil

1. Introduction

Water erosion, in addition to drought, flooding, salinity, contamination by heavy metals, waste disposal and peat-bogs decay, is one of the forms of earth surface degradation. Ref. [1] carried out simulations of water erosion intensity caused by various land use scenarios in the highly eroded mountain Małny stream basin located in the Western Carpathians. Ref. [2] analyzed soil erosion in China between 1980 and 2010, incorporated with landform, slope, vegetation coverage, land use and remote sensing images. This process takes place especially in loess areas all over the world [3–7]. Ref. [8] carried out a laboratory experiment devoted to the influence of drying and rewetting cycles on respiratory processes in organic soil. Ref. [9] carried out investigations on salinity problems connected with landfill of the Cracow Soda Plant. Ref. [10] presented the state of the art connected with drivers, indicators and monitoring, modeling and mapping methods for salinity of soil. Refs. [11,12] elaborated the dependence of salinity and sodicity levels on irrigation water quality, using a numerical approach. Ref. [13] investigated the influence of soil salinity on microorganisms and respiratory responses. Ref. [14] presented the optimization method in optimizing the parameters of the salinity stress reduction function, establishing the root-water-uptake model and simulating soil water flow under the salinity stress condition. Ref. [15] studied the concentrations of heavy metals in water, sediment, zooplankton and fish in the coastal waters of Kalpakkam, near a nuclear power plant. Ref. [16] investigated the significance of halophytes in conditions of high salinity and their role in the process of phytoremediation

of heavy metals. Ref. [17] examined the water retention ability of chosen industrial wastes taken from landfills. Ref. [18] determined physical, hydrophysical and chemical properties of the upper layer of peat soil on post-extracted areas. One of the soil properties regarded in water erosion evaluation is saturated hydraulic conductivity [19–21]. It is taken into account as a criteria for hydrologic group identification for CN parameter and maximum potential basin retention determination [22]. It is one of the parameters for water transport models in the unsaturated zone [23] and depends mainly on: texture, bulk density and organic matter content [7,24]. This soil property is characterized by particular high spatial variability [25–29]. There are many methods for saturated hydraulic conductivity determination. In general, the methods can be classified as: laboratory, field and empirical ones [30]. The laboratory and fields methods are the most accurate, but they are time and cost consuming. In turn, the empirical methods are quick and easy, as usually they require only knowledge of the grain size distribution curve and some physical properties of soil and water (for example, total porosity and water specific density) [30–36]. They are grouped in three categories. The simplest are based only on some effective diameters, taken from grain size distribution curve. The second ones, apart from effective diameters, take into account chosen soil physical properties, most often porosity. The third ones are based apart above properties, on physical properties of water, such as: specific density or viscosity [37]. In the literature, the methods are most commonly reported as the pedotransfer functions (PTF) [24,38–45]. The pedotransfer functions can be regarded as wider term than empirical functions. This term was proposed for the first time by [46], although such an approach depends on the estimation of soil properties from other more easily measurable soil properties [47]. This had been known since the early 20th century [48]. The easy measurable parameters are called predictors. They are: sand, silt and clay fractions content [49–51], organic matter or organic carbon content and bulk density [12,50,52–55]. Explaining parameters are most often: hydraulic parameters (hydraulic conductivity, water retention), solute transport parameters (preferential flow, solute transport), thermal parameters (thermal conductivity) and biogeochemical parameters (adsorption isotherm, carbon stocks) [47].

2. Material and Methods

2.1. Pedotransfer Functions

In this work there were used 15 pedotransfer functions for determination of saturated hydraulic conductivity:

Method 1—Hazen [36]:

$$K_s = c \cdot d_{10}^2 [\text{m} \cdot \text{day}^{-1}]$$

where:

K_s —saturated hydraulic conductivity [$\text{m} \cdot \text{day}^{-1}$]

d_{10} —effective grain size, soil particle diameter [mm] such that 10% of all particles are finer by weight.

c —a constant that varies from 1.0 to 1.5 if K_s is expressed in $\text{cm} \cdot \text{s}^{-1}$ in original method proposed by Hazen; in the work it was taken according to Lange as: $c = [400 + 40 \cdot (n - 26)]$, where n is total porosity (%).

Method 2—Hazen—Tkaczukowa [56]:

$$K_s = 864 \cdot \frac{0.0093}{a^2} \cdot d_{10}^2 [\text{m} \cdot \text{day}^{-1}]$$

where:

a —content of particles of diameter $d < 0.001$ mm [-],

d_{10} —as above.

Method 3—USBR [57]:

$$K_s = 86,400 \cdot 0.0036 d_{20}^{2.3} [\text{m} \cdot \text{day}^{-1}]$$

where:

d_{20} —effective grain size soil particle diameter [mm] such that 20% of all particles are finer by weight.

Method 4—Saxton et al. [44,58]:

$$K_s = e^{12.012 - 0.0755 \cdot (S_i) + (-3.895 + 0.0367 \cdot (S_i) - 0.1103 \cdot (C)) + \frac{0.00087546 \cdot (C)^2}{\theta_s}} [\text{m} \cdot \text{day}^{-1}]$$

where:

C —clay fraction content (<0.002 mm) [%],

S_i —silt fraction content (0.05–0.002 mm) [%],

θ_s —saturated soil moisture [$\text{m}^3 \cdot \text{m}^{-3}$], calculated as: $\theta_s = 0.332 - 0.0007251 \cdot S + 0.1276 \cdot \log(C)$.

Method 5—Kozeny—Carman [31]:

$$K_s = \left(\frac{\gamma}{\mu} \right) \cdot \left(\frac{1}{C_{KC} \cdot S_0^2} \right) \cdot \left(\frac{e^3}{1+e} \right) [\text{m} \cdot \text{day}^{-1}]$$

where:

γ —specific density of water [$\text{Mg} \cdot \text{m}^{-3}$],

μ —dynamic liquid viscosity coefficient [$\text{m} \cdot \text{s}^{-2}$],

e —void ratio [-],

S_0 —specific area [cm^{-1}], in the work it was measured by gravimetric method (glycerine as absorber)

C_{KC} —Kozeny-Carman constant, taken most often as 5.

Method 6—Krüger [37]:

$$K_s = 322 \cdot \frac{n}{(1-n)^2} \cdot d_e^2 [\text{m} \cdot \text{day}^{-1}]$$

where:

n —total porosity (-),

d_e —effective diameter (mm) calculated as: $d_e = \frac{100}{\sum_1^N \frac{a_i}{d_i}}$, where: N —number of fraction,

a_i —percentage of following fractions in texture, d_i —grain diameter within following fractions from 1 to N (mm), calculated as: $d_i = \frac{d_y + d_x}{2}$, where: d_y and d_x —lower and upper diameter of following fractions from 1 to N .

Method 7—Terzaghi [34,59]:

$$K_s = \frac{C}{\eta} \cdot \left(\frac{n - 0.13}{\sqrt[3]{1-n}} \right)^2 \cdot d_{10}^2 \cdot (1 + 0.034 \cdot t) [\text{m} \cdot \text{day}^{-1}]$$

where:

C —coefficient depending on shape of particles, equal to 10.48 for round and 6.02 for sharp edge particles [-],

h —viscosity coefficient [$\text{Pa} \cdot \text{s}$],

n —as above,

d_{10} —as above,

t —temperature of water [$^{\circ}\text{C}$]

Method 8—Chapuis [32]:

$$K_s = 864 \cdot 2.4622 \cdot d_{10}^2 \cdot \left(\frac{e^3}{1+e} \right)^{0.7825} \text{ [m} \cdot \text{day}^{-1}]$$

where:

e —void ratio [-],
 d_{10} —as above.

Method 9—Seelheim [60]:

$$K_s = 864 \cdot 0.357 \cdot d_{50}^2 \text{ [m} \cdot \text{day}^{-1}]$$

where:

d_{50} —effective diameter[mm], such that 50% of all particles are finer by weight.

Method 10—NAVFAC [32,61]:

$$K_s = 864 \cdot 10^{1.291 \cdot e - 0.6435} \cdot d_{10}^{10^{0.5504 - 0.2937 \cdot e}} \text{ [m} \cdot \text{day}^{-1}]$$

where:

e —void ratio [-],
 d_{10} —as above.

Method 11—Sauerbrej [57]:

$$K_s = \beta \cdot \frac{n^2}{(1-n)^2} \cdot d_{20}^2 \text{ [m} \cdot \text{day}^{-1}]$$

where:

β —empirical coefficient [-] depending on dimension and grain size homogeneity, it takes value between 1150 and 3010 (usually 2880–3010, in the work it was taken as 2945,
 d_{20} —as above,
 n —as above.

Method 12—Slichter [62]:

$$K_s = 86,400 \cdot 8.83 \cdot d_{10}^2 \cdot \frac{1}{\mu} \cdot m \text{ [m} \cdot \text{day}^{-1}]$$

where:

d_{10} —as above,
 m —coefficient depending on porosity, $m = 0.0039 \cdot n - 0.0012$, where n is total porosity [-],
 μ —dynamic viscosity of water [Pa·s].

Method 13—Furnival and Wilson [63]:

$$K_s = 9.5 - 1.471 \cdot BD^2 - 0.688 \cdot OM + 0.0369 \cdot OM^2 - 0.332 \cdot \ln(C + S_i) \text{ [m} \cdot \text{day}^{-1}]$$

where:

BD —bulk density [$\text{Mg} \cdot \text{m}^{-3}$]
 OM —organic matter content [%],
 C —clay fraction content [%],
 S_i —silt fraction content [%].

Method 14—MRA (multiple regression analysis).

Model of MRA was carried out based on data published by Ryczek et al. (2017)

$$K_s = 3.61216 + 0.04474 \cdot S + 0.01300 \cdot S_i - 2.42722 \cdot C - 3.28861 \cdot n \text{ [m} \cdot \text{day}^{-1}]$$

where:

S —sand fraction (2–0.05 mm) content [%],
 S_i —silt fraction (0.05–0.002 mm) content [%],
 C —clay fraction (<0.002 mm) content [%],
 n —as above [-].

Regression coefficients were calculated in Statistica program release 13.5.

Method 15—ANN (Artificial Neural Networks) [43,64,65].

In the work we used the ANN model MLP 11-11-1, as described by [66]. The input data were 11 soil parameters: content of clay, silt and sand fractions, as well as total porosity, organic matter content and effective diameters: d_{10} , d_{20} , d_{50} , d_{60} i d_{90} , and bulk and solid phase density.

2.2. Soil Properties

The methods for determination of soil properties were presented in Table 1.

Table 1. Methods for determination of soil properties.

Soil Property	Methods
texture	the Casagrande sedimentation and sieve methods; classification of fractions and granular groups was carried out according to USDA (United States Department of Agriculture)
total porosity (n)	$n = 1 - BD \cdot SD^{-1}$, where: BD —bulk density, measured by means of ring method, SD —specific density, measured by means of pycnometric method
void ratio (e)	$e = n(1 - n)^{-1}$
saturated hydraulic conductivity (K_s)	doubling infiltrometer
organic matter content (OM)	the Tiurin method

2.3. Statistical Analysis

The adjustment of the results obtained by means of the chosen pedotransfer functions to the ones obtained using the double ring method was evaluated by means of some statistical parameters, as [40,67]:

- mean error of prognosis (MEP)

$$MEP = \frac{1}{n} \cdot \sum_{i=1}^n (C_i^m - C_i^p)$$

- root of mean square error ($RMSE$)

$$RMSE = \sqrt{\frac{1}{n} \cdot \sum_{i=1}^n (C_i^m - C_i^p)^2}$$

- mean percentage error (MPE)

$$MPE = \frac{1}{n} \cdot \sum_{i=1}^n \frac{C_i^m - C_i^p}{C_i^m} \cdot 100$$

- model efficiency (ME) [41,45]

$$ME = 1 - \frac{\sum_{i=1}^n (C_i^m - C_i^p)^2}{\sum_{i=1}^n (C_i^m - \bar{C})^2}$$

where:

C_i^m —measured values,

C_i^p —simulated values,

n —number of data,

\bar{C} —mean measured value.

Statistical significance of differences between pedotransfer functions were checked by means of LSD_{Tukey} (least significant differences by Tukey's test).

2.4. Investigated Site

The field experiment was carried out on the evidence plot 647, precinct Brzeźnica, evidence unit Rudnik (community), Silesia voivodship, Racibórz district (Figure 1), belonging to the Agriculture-Industry Enterprise in Racibórz, LC. The experiment site belongs to the mesoregion Racibórz Valley [68,69]. According to the Gumiński agricultural-climatic provinces, the site belongs to province Sub Sudety—XVIII. Samples were taken from 9 points, located in regular squares network (Figure 2). The investigated site is characterized by high slope attaining 20° . It has been used as arable land, under maize and earlier under winter wheat. According to texture (15% of sand, 75% of silt, 10% of clay), soil is classified as: silt loam (SiL) [53]. It is the typical loamy loess and undergoes high water erosion.

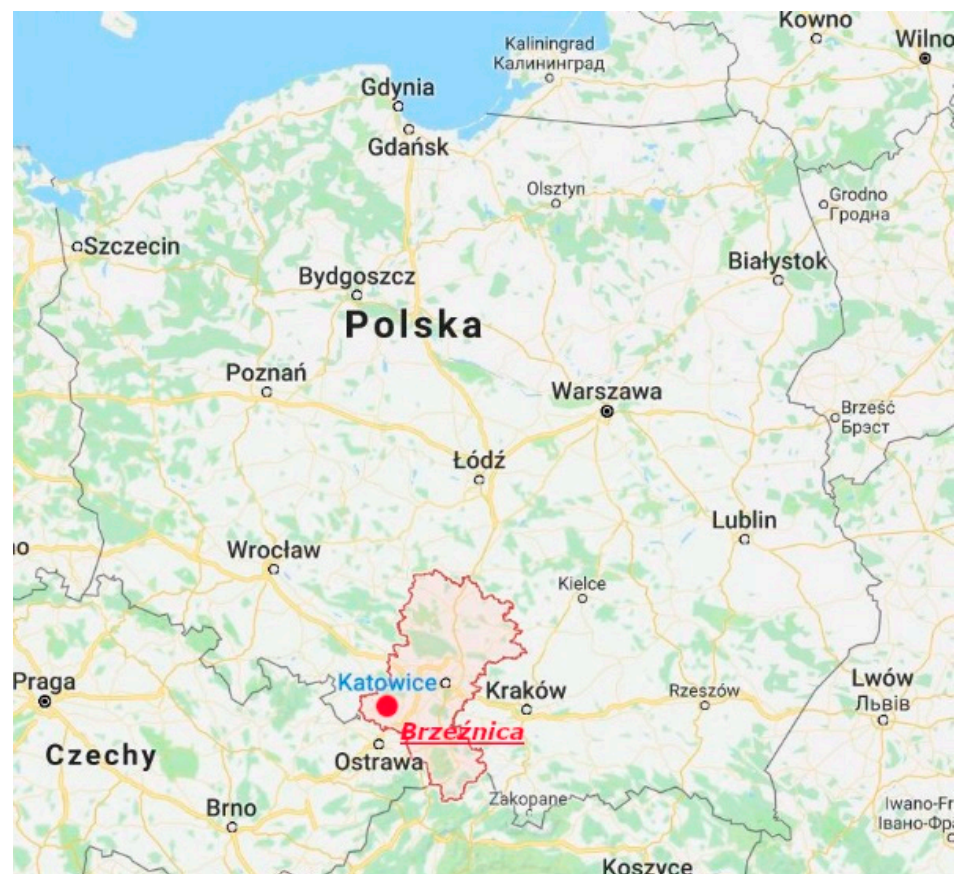


Figure 1. Location of the investigated site (source: www.google.pl/maps (accessed on 20 November 2022)).



Figure 2. Location of experiment points (source: www.googlemap.pl (accessed on 20 November 2022)).

3. Results and Discussion

In Table 2 there are presented values of some statistical measures of soil parameters used for calculation of saturated hydraulic conductivity by use of pedotransfer functions. Regarding texture, soil on the investigated site is classified as silt loam (SiL). Effective diameter d_{10} varied from $1.7 \cdot 10^{-3}$ to $3.0 \cdot 10^{-3}$ mm, d_{20} between $4.5 \cdot 10^{-3}$ and $8.0 \cdot 10^{-3}$ mm, while d_{50} between $2.8 \cdot 10^{-3}$ mm and $3.8 \cdot 10^{-2}$ mm. Values of organic matter fluctuated between 0.85 and 1.35%, while total porosity between 0.394 and 0.481. Bulk density attained values between 1.41 and $1.57 \text{ Mg} \cdot \text{m}^{-3}$. Values of saturated hydraulic conductivity K_s for analyzed points fluctuated between $3.25 \cdot 10^{-2}$ and $8.72 \cdot 10^{-2} \text{ m} \cdot \text{day}^{-1}$.

Table 2. Statistical values of parameters for determination of saturated hydraulic conductivity by means of the pedotransfer functions.

Soil Parameter	Statistical Parameters				
	V_{min}	V_{max}	\bar{x}	σ_{n-1}	V (%)
C [%]	5	12	10	2	20.0
S_i [%]	70	79	75	3	4.0
S [%]	13	18	15	2	13.3
d_{10} [mm]	$1.7 \cdot 10^{-3}$	$3.0 \cdot 10^{-3}$	$2.1 \cdot 10^{-3}$	$5.0 \cdot 10^{-4}$	23.7
d_{20} [mm]	$4.5 \cdot 10^{-3}$	$8.0 \cdot 10^{-3}$	$6.2 \cdot 10^{-3}$	$1.2 \cdot 10^{-3}$	19.4
d_{50} [mm]	$9.6 \cdot 10^{-3}$	$2.8 \cdot 10^{-2}$	$2.2 \cdot 10^{-2}$	$5.0 \cdot 10^{-3}$	22.7
d_{60} [mm]	$2.8 \cdot 10^{-3}$	$3.8 \cdot 10^{-2}$	$2.5 \cdot 10^{-2}$	$1.0 \cdot 10^{-2}$	40.0
d_{90} [mm]	$6.0 \cdot 10^{-2}$	$8.5 \cdot 10^{-2}$	$7.3 \cdot 10^{-2}$	$8.2 \cdot 10^{-3}$	11.2
d_e [mm]	$1.1 \cdot 10^{-2}$	$1.8 \cdot 10^{-2}$	$1.3 \cdot 10^{-2}$	$2.2 \cdot 10^{-3}$	16.8
a [-]	0.02	0.06	0.04	0.01	25.0
OM [%]	0.85	1.35	1.06	0.15	13.9
n [-]	0.394	0.481	0.433	0.031	7.1
e [-]	0.650	0.927	0.769	0.097	12.6
BD [$\text{Mg} \cdot \text{m}^{-3}$]	1.41	1.57	1.50	0.06	4.1
K_s [$\text{m} \cdot \text{day}^{-1}$]	$3.25 \cdot 10^{-2}$	$8.72 \cdot 10^{-2}$	$6.59 \cdot 10^{-2}$	$1.96 \cdot 10^{-2}$	29.7

Meanings: C —clay fraction (<0.002 mm) content, S_i —silt fraction (0.05–0.002 mm) content, S —sand fraction (2–0.05 mm) content, d_e —proper effective diameter [mm], a —content of particles below 0.001 mm, OM —organic matter content, n —total porosity, e —void ratio, BD —bulk density, K_s —saturated hydraulic conductivity.

Table 3 presents some statistical measures for saturated hydraulic conductivity determined by one of the fifteen pedotransfer functions. Generally, the obtained mean values were between $9.10 \cdot 10^{-4}$ and $4.59 \cdot 10^0$ m·day⁻¹.

Table 3. Statistical parameters of the saturated hydraulic conductivity obtained for the chosen pedotransfer functions.

Method	Statistical Parameters				
	V_{min}	V_{max}	\bar{x}	σ_{n-1}	V
	(m·day ⁻¹)				(%)
1	$2.71 \cdot 10^{-3}$	$9.83 \cdot 10^{-3}$	$5.04 \cdot 10^{-3}$	$2.50 \cdot 10^{-3}$	49.6
2	$6.45 \cdot 10^{-3}$	$1.69 \cdot 10^{-1}$	$4.22 \cdot 10^{-2}$	$5.22 \cdot 10^{-2}$	123.6
3	$1.25 \cdot 10^{-3}$	$4.68 \cdot 10^{-3}$	$2.73 \cdot 10^{-3}$	$1.15 \cdot 10^{-3}$	42.1
4	$1.21 \cdot 10^{-2}$	$2.22 \cdot 10^{-2}$	$1.59 \cdot 10^{-2}$	$3.23 \cdot 10^{-3}$	20.3
5	$2.62 \cdot 10^{-2}$	$1.24 \cdot 10^{-1}$	$6.51 \cdot 10^{-2}$	$3.28 \cdot 10^{-2}$	50.4
6	$4.36 \cdot 10^{-2}$	$1.27 \cdot 10^{-1}$	$7.71 \cdot 10^{-2}$	$2.67 \cdot 10^{-2}$	34.6
7	$1.10 \cdot 10^{-2}$	$4.16 \cdot 10^{-2}$	$2.14 \cdot 10^{-2}$	$1.06 \cdot 10^{-2}$	49.5
8	$1.83 \cdot 10^{-3}$	$1.15 \cdot 10^{-2}$	$4.90 \cdot 10^{-3}$	$4.11 \cdot 10^{-3}$	83.9
9	$8.91 \cdot 10^{-2}$	$4.45 \cdot 10^{-1}$	$2.54 \cdot 10^{-1}$	$9.57 \cdot 10^{-2}$	37.6
10	$6.20 \cdot 10^{-4}$	$2.34 \cdot 10^{-2}$	$5.87 \cdot 10^{-3}$	$7.28 \cdot 10^{-3}$	123.9
11	$2.72 \cdot 10^{-2}$	$1.24 \cdot 10^{-1}$	$7.05 \cdot 10^{-2}$	$3.07 \cdot 10^{-2}$	43.5
12	$9.10 \cdot 10^{-4}$	$3.87 \cdot 10^{-3}$	$2.00 \cdot 10^{-3}$	$9.90 \cdot 10^{-4}$	49.4
13	$3.70 \cdot 10^0$	$4.59 \cdot 10^0$	$4.05 \cdot 10^0$	$3.14 \cdot 10^{-1}$	7.7
14	$2.63 \cdot 10^{-2}$	$4.74 \cdot 10^{-1}$	$2.05 \cdot 10^{-1}$	$1.28 \cdot 10^{-1}$	62.7
15	$5.20 \cdot 10^{-2}$	$5.21 \cdot 10^{-2}$	$5.21 \cdot 10^{-2}$	$3.00 \cdot 10^{-5}$	0.1

The analysis of variance was introduced in Table 4, while Table 5 presents statistically uniform groups regarding statistical essentiality. Method 13 (Fournivaland Wilson) showed statistically essential difference in relation to the other methods. In turn, between method 9 (Seelheim) and 14 (multiple regression) there is no statistically essential difference. Between method 14 (multiple regression) and the remaining following methods there is no statistical essential difference.

Table 4. Analysis of variance.

Variability Source	Squares Sum	Freedom Degrees	Mean Square
Points	0.111	8	
Methods	134.509	14	9.608
Error	0.917	112	0.008
Total	135.537	134	

Calculation of the LSD by the Tukey test: the Tukey distribution q for $\alpha = 0.05$, $\nu = 112$ and $m = 15$ is equal 4.91, standard deviation of arithmetic mean: $s_x = 0.03016$. LSD = 0.148.

In Table 6 there are presented results of statistical analysis of comparison of results obtained by means of field direct methods with the ones obtained by means of the chosen pedotransfer methods. The results show that the method 1 (Hazen), 3 (USBR), 4 (Saxton), 7 (Tezaghi), 8 (Chapuis), 9 (Seelheim), 10 (Chapuis-NAVFAC), 12 (Slichter), 13 (Furnival) and 14 (multiple regression) gave statistically essential differences in relation to the results obtained by means of the field method. Comparing, in turn, percentage differences, the least one showed method 5 (Kozeny-Carman, underestimation attaining 1.4%), and the highest showed method 13 (Furnival and Wilson, overestimation attained as many as 6036.4%).

Table 5. Analysis of essential differences between results of determination by means of the pedotransfer functions.

Method	Mean [$\text{m}\cdot\text{day}^{-1}$]	Homogenous Groups
13	$4.05\cdot 10^0$	a
9	$2.54\cdot 10^{-1}$	b
14	$2.05\cdot 10^{-1}$	bc
6	$7.70\cdot 10^{-2}$	c
11	$7.05\cdot 10^{-2}$	c
5	$6.51\cdot 10^{-2}$	c
15	$5.21\cdot 10^{-2}$	c
2	$4.22\cdot 10^{-2}$	c
7	$2.14\cdot 10^{-2}$	c
4	$1.59\cdot 10^{-2}$	c
10	$6.92\cdot 10^{-3}$	c
1	$5.04\cdot 10^{-3}$	c
8	$3.39\cdot 10^{-3}$	c
3	$2.73\cdot 10^{-3}$	c
12	$2.00\cdot 10^{-3}$	c

Mean value of saturated hydraulic conductivity obtained by means of double-ring method was: $6.59\cdot 10^{-2} \text{ m}\cdot\text{day}^{-1}$ with standard deviation $1.96\cdot 10^{-2} \text{ m}\cdot\text{day}^{-1}$, and variation coefficient 29.7%.

Table 6. Values of t-Student test between results obtained by means of the pedotransfer functions with the ones obtained by means of measured data.

Method	Test t-Student Value	Critical Value $t_{0,05}$	Difference % **
1	-10.567 *		92.4
2	-0.743		36.1
3	-11.273 *		95.0
4	-8.477 *		75.9
5	-0.030		1.4
6	0.677		-16.7
7	-5.278 *		67.6
8	-11.061 *		94.9
9	3.286 *		-284.8
10	-8.396 *		89.5
11	0.251	2.228	-6.8
12	-11.426 *		97.0
13	21.423 *		-6036.4
14	-2.452 *		-210.6
15	1.812		21.1

* differences are statistically essential, ** positive values show underestimation of the pedotransfer function in relation to the measured values, while negative values show overestimation.

For the purpose to choose the best function simulating saturated hydraulic conductivity for the loess soil, the various model efficiency measures were used (Table 7). Values of correlation coefficient r for pedotransfer functions fluctuated between 0.059 and 0.708. Only for methods 2nd (Hazen-Tkaczukowa), 4th (Saxton), 10th (NAVFAC) and 15th (ANN) coefficients were statistically essential for confidence level 0.01. The best accordance with the field double-ring method regarding correlation coefficient had the 15th (ANN) method, while the most abandoning ones were 11th (Sauerbreij) and 12th (Slichter) functions. Results obtained for MEP showed that maximum underestimation attained $2.18\cdot 10^{-2}$, for 15th (ANN) function, while little overestimation took place for 11th (Sauerbreij) function. Mean percentage error MPE shows good results of estimation for 2nd (Hazen-Tkaczukowa) function. Its value was 6.2%. Extreme bad adjustment had 13th (Furnival and Wilson) (as many as -5774.6%) function. Root of mean square error $RMSE$ attained the highest value for 13th (Furnival and Wilson) function ($3.99\cdot 10^0\cdot 10^0 \text{ m}\cdot\text{day}^{-1}$). The best results attained 15th (ANN) function. Analysis of homogeneity of mean values (Table 4) using the Tukey's

test LSD_{Tukey} showed that the 13th (Furnival and Wilson) method differed statistically in comparison to other functions (Table 8). Functions 9th (Seelheim) and 14th (MRA) did not differ between them and differed statistically from the remaining methods.

Table 7. Model efficiency measures.

Model	Efficiency Measures				
	MEP [m·day ⁻¹]	RMSE [m·day ⁻¹]	MPE [%]	ME [-]	r [-]
1	6.09·10 ⁻²	6.40·10 ⁻²	90.8	−10.973	0.440
2	2.37·10 ⁻²	6.69·10 ⁻²	6.2	−12.070	0.630 *
3	6.32·10 ⁻²	6.60·10 ⁻²	94.9	−11.743	0.501
4	5.00·10 ⁻²	5.42·10 ⁻²	71.6	−7.577	0.716 *
5	8.22·10 ⁻⁴	3.94·10 ⁻²	−14.2	−3.540	0.221
6	−1.11·10 ⁻²	3.88·10 ⁻²	−38.3	−3.414	0.439
7	4.46·10 ⁻²	5.08·10 ⁻²	61.2	−6.547	0.416
8	6.25·10 ⁻²	6.54·10 ⁻²	94.0	11.496	0.300
9	−1.88·10 ⁻¹	2.12·10 ⁻¹	−355.5	−131.000	0.361
10	5.51·10 ⁻²	5.73·10 ⁻²	85.1	−8.585	0.549 *
11	−4.54·10 ⁻³	3.55·10 ⁻²	−22.4	−2.692	0.059
12	7.19·10 ⁻²	7.40·10 ⁻²	97.2	−13.436	0.059
13	−3.98·10 ⁰	3.99·10 ⁰	−5774.6	−41,907.886	0.156
14	−1.31·10 ⁻¹	1.77·10 ⁻¹	−185.5	81.138	0.206
15	2.18·10 ⁻²	2.81·10 ⁻²	24.0	−1.080	0.708 *

*—statistically essential for confidence level 0.1.

Table 8. Values of parameters of spatial distribution.

Methods	Mean Value	Standard Deviation	Variability Coefficient
1	5.04·10 ⁻³	2.50·10 ⁻³	49.7
2	4.22·10 ⁻²	5.21·10 ⁻²	123.6
3	2.73·10 ⁻³	1.15·10 ⁻³	42.1
4	1.59·10 ⁻²	3.24·10 ⁻³	20.3
5	6.51·10 ⁻²	3.27·10 ⁻²	50.3
6	7.70·10 ⁻²	2.66·10 ⁻²	34.5
7	2.14·10 ⁻²	1.06·10 ⁻²	49.4
8	3.39·10 ⁻³	1.68·10 ⁻³	49.4
9	2.54·10 ⁻¹	9.58·10 ⁻²	37.7
10	6.92·10 ⁻³	7.17·10 ⁻³	103.6
11	7.05·10 ⁻²	3.07·10 ⁻²	43.5
12	2.00·10 ⁻³	9.90·10 ⁻⁴	49.4
13	4.05·10 ⁰	3.12·10 ⁻¹	7.7
14	2.05·10 ⁻¹	1.28·10 ⁻¹	62.7
15	5.21·10 ⁻²	2.07·10 ⁻⁵	0.0

4. Conclusions

1. The LSD analysis showed that the Fournival and Wilson method, based on texture and total porosity differs statistically for investigated site from the other methods. In turn, between the Seelheim (based on texture only) and multiple regression methods there is not a statistical difference. Between the Seelheim method and the other ones there are not a statistically essential difference;
2. The t-Student analysis showed that the methods: Hazen, USBR, Saxton, Seelheim (based only on texture), Chapuis, NAVFAC, Furnival and Wiliam, multiple regression (based on texture and total porosity), and Slichter and Tezaghi (based on texture, total porosity and water properties)gave statistically essential differences in comparison to the results obtained by the field method. The remaining method does not differ statistically from the field method;

3. Comparing the percentage differences, the lowest showed the Kozeny-Carman method, in which underestimation in relation to the field method was 1.4%. In turn, the highest difference was in the case of the Furnival and Wilson, in which overestimation was as many as 5.4%. The lowest differences were in the case of the methods where total porosity was taken into account;
4. The highest spatial variability was for the Hazen and Tkaczukowa methods, where variability coefficient was 123.6%. In turn, the artificial neural network method was characterized by a lack of variability.

Author Contributions: Conceptualization, A.P. and M.R.; methodology, A.P. and M.R.; validation, E.K., L.L.; formal analysis, M.R.; resources M.R. and E.K.; writing—original draft preparation, M.R. and A.P.; writing—review and editing, A.P. and M.R.; supervision, E.K. and L.L.; project administration, A.P.; funding acquisition, A.P. and E.K. All authors have read and agreed to the published version of the manuscript.

Funding: The publication was co-financed from the subsidy granted to the Cracow University of Economics—Project nr 28/GGR/2021/POT.

Institutional Review Board Statement: Not applicable.

Informed Consent Statement: Not applicable.

Conflicts of Interest: The authors declare no conflict of interest.

References

1. Halecki, W.; Kruk, E.; Ryczek, M. Loss of top soil and soil erosion by water in agricultural areas: A multi-criteria approach for various land use scenarios in the Western Carpathians using a SWAT model. *Land Use Policy* **2018**, *73*, 363–372. [[CrossRef](#)]
2. Wang, X.; Zhao, X.; Zhang, Z.; Yi, L.; Zuo, L.; Wen, Q.; Liu, F.; Xu, J.; Hu, S.; Liu, B. Assessment of soil erosion change and its relationships with land use/cover change in China from the end of the 1980s to 2010. *Catena* **2016**, *137*, 256–268. [[CrossRef](#)]
3. Cadaret, E.M.; McGwire, K.C.; Nouwakpo, S.K.; Weltz, M.A.; Saito, L. Vegetation canopy cover effects on sediment erosion processes in the Upper Colorado River Basin Mancos Shale formation, Price, Utah, USA. *Catena* **2016**, *147*, 334–344. [[CrossRef](#)]
4. Cao, T.; She, D.; Zhang, X.; Yang, Z.; Wang, G. Pedotransfer functions developed for calculating soil saturated hydraulic conductivity in check dams on the Loess Plateau in China. *Vadose Zone J.* **2022**, *21*, 20217. [[CrossRef](#)]
5. Evrarda, O.; Nordb, G.; Cerdanc, O.; Souchère, V.; Le Bissonnais, Y.; Bonté, P. Modelling the impact of land use change and rainfall seasonality on sediment export from an agricultural catchment of the northwestern European loess belt. *Agric. Ecosyst. Environ.* **2010**, *138*, 83–94. [[CrossRef](#)]
6. Lia, P.; Mua, X.; Holden, J.; Wud, Y.; Irvine, B.; Wanga, F.; Gao, P.; Zhao, G.; Sun, W. Comparison of soil erosion models used to study the Chinese Loess Plateau. *Earth-Sci. Rev.* **2017**, *170*, 17–30. [[CrossRef](#)]
7. Yang, G.; Xu, Y.; Huo, L.; Wang, H. Analysis of Temperature Effect on Saturated Hydraulic Conductivity of the Chinese Loess. *Water* **2022**, *14*, 1327. [[CrossRef](#)]
8. Li, J.T.; Wang, J.J.; Zeng, D.H.; Zhao, S.Y.; Huang, W.L.; Sun, X.K.; Hu, J. The influence of drought intensity on soil respiration during and after multiple drying-rewetting cycles. *Soil Biol. Biochem.* **2018**, *127*, 82–89. [[CrossRef](#)]
9. Boroń, K.; Klatka, S.; Ryczek, M.; Zając, E. Reclamation and cultivation of Cracow Soda plant Lagoons. In *Construction for Sustainable Environment*; Sarsby, R., Meggyes, T., Eds.; CRC Press Taylor & Francis Group: London, UK, 2010; pp. 245–250.
10. Daliakopoulos, I.N.; Tsanis, I.; Koutroulis, A.; Kourgialas, N.; Varouchakis, A.; Karatzas, G.; Ritsema, C. The threat of soil salinity: A European scale review. *Sci. Total Environ.* **2016**, *573*, 727–739. [[CrossRef](#)]
11. Mau, Y.; Porporato, A. A dynamical system approach to soil salinity and sodicity. *Adv. Water Resour.* **2015**, *83*, 68–76. [[CrossRef](#)]
12. Mau, Y.; Porporato, A. Optimal control solutions to sodic soil reclamation. *Adv. Water Resour.* **2016**, *91*, 37–45. [[CrossRef](#)]
13. Rath, K.M.; Maheshwari, A.; Rousk, J. The impact of salinity on the microbial response to drying and rewetting in soil. *Soil Biol. Biochem.* **2017**, *108*, 17–26. [[CrossRef](#)]
14. Wanga, L.; Shi, J.; Zuo, Q.; Zhang, W.; Zhuc, X. Optimizing parameters of salinity stress reduction function using the relationship between root-water uptake and root nitrogen mass of winter wheat. *Agric. Water Manag.* **2012**, *104*, 142–152. [[CrossRef](#)]
15. Achary, M.S.; Satpathy, K.; Panigrahi, S.; Mohanty, A.; Padhi, R.; Biswas, S.; Prabhu, R.; Vijayalakshmi, S.; Panigrahy, R. Concentration of heavy metals in the food chain components of the nearshore coastal waters of Kalpakkam, southeast coast of India. *Food Control* **2017**, *72*, 232–243. [[CrossRef](#)]
16. VanOosten, M.J.; Maggio, A. Functional biology of halophytes in the phytoremediation of heavy metal contaminated soils. *Environ. Exp. Bot.* **2015**, *111*, 135–146. [[CrossRef](#)]
17. Klatka, S.; Malec, M.; Ryczek, M.; Kruk, E.; Zając, E. Evaluation of retention ability of chosen industrial wastes. *Acta Sci. Pol. Form. Circumiectus* **2016**, *15*, 53–60. [[CrossRef](#)]

18. Zając, E.; Zarzycki, J.; Ryczek, M. Degradation of peat surface on an abandoned post-extracted bog and implications for re-vegetation. *Appl. Ecol. Environ. Res.* **2018**, *16*, 3363–3380. [[CrossRef](#)]
19. El-Hames, A.S. An empirical method for peak discharge prediction in ungauged arid and semi-arid region catchments based on morphological parameters and SCS curve number. *J. Hydrol.* **2012**, *456–457*, 94–100. [[CrossRef](#)]
20. Sanzeni, A.; Colleselli, F.; Grazioli, D. Specific surface and Hydraulic Conductivity of Fine-Grained Soils. *J. Geotech. Geoenvironmental Eng.* **2013**, *139*, 892. [[CrossRef](#)]
21. Tyagi, J.V.; Mishra, S.K.; Singh, R.; Singh, V.P. SCS-CN based time-distributed sediment yield model. *J. Hydrol.* **2008**, *352*, 388–403. [[CrossRef](#)]
22. USDA. *Urban Hydrology for Small Watersheds*; Technical Release, 55; U.S. Department of Agriculture, Natural Resources Conservation Service, Conservation Engineering Division: Washington, DC, USA, 1986.
23. Tietje, O.; Hennings, V. Accuracy of the saturated hydraulic conductivity prediction by pedo-transfer functions compared to the variability within FAO textural classes. *Geoderma* **1996**, *69*, 71–84. [[CrossRef](#)]
24. Abdelbaki, A.M. Selecting the most suitable pedotransfer functions for estimating saturated hydraulic conductivity according to the available soil inputs. *Ain Eng. J.* **2021**, *12*, 2603–2615. [[CrossRef](#)]
25. Ke, X.; Liu, P.; Wang, W.; Li, J.; Niu, F.; Gao, Z.; Kong, D. Spatial variability of the vertical saturated hydraulic conductivity of sediments around typical thermokarst lakes. *Geoderma* **2023**, *429*, 116230. [[CrossRef](#)]
26. Klatka, S.; Ryczek, M.; Boroń, K. Water characteristics curves of soils degraded by coal mine industry. *Ochr. Sr. I Zasobów Nat.* **2010**, *42*, 130–135.
27. Klatka, S.; Malec, M.; Ryczek, M. Analysis of Spatial Variability of Selected Soil Properties in the Hard Coal Post-Mining Area. *J. Ecol. Eng.* **2019**, *20*, 185–193. [[CrossRef](#)]
28. Regalado, C.M.; Muñoz-Carpena, R. Estimating the saturated hydraulic conductivity in a spatially variable soil with different permeameters: A stochastic Kozeny–Carman relations. *Soil Tillage Res.* **2004**, *77*, 189–202. [[CrossRef](#)]
29. Rienzner, M.; Gandolfi, C. Investigation of spatial and temporal variability of saturated soil hydraulic conductivity at the field-scale. *Soil Tillage Res.* **2014**, *135*, 28–40. [[CrossRef](#)]
30. Jabro, J. Estimation of saturated conductivity of solis from particle size distribution and bulk density date. *Trans. Am. Soc. Agric. Eng.* **1992**, *35*, 557–560. [[CrossRef](#)]
31. Carrier, D. Goodbye, Hazen; Hello, Kozeny-Carman, Technical notes. *J. Geotech. Geoenvironmental Eng.* **2003**, *129*, 1054–1056. [[CrossRef](#)]
32. Chapuis, R. Predicting the Saturated Hydraulic Conductivity of Natural Soils. *Geotech. News* **2008**, 47–50.
33. Kruk, E.; Klapa, P.; Ryczek, M.; Ostrowski, K. Comparison of the USLE to pographical factor parameter generated by various DE Melaboration methods on loess lope. *Remote Sens.* **2020**, *12*, 3540. [[CrossRef](#)]
34. Odong, J. Evaluation of empirical formulae for determination of hydraulic conductivity based on grain-size analysis. *J. Am. Sci.* **2007**, *3*, 54–60.
35. Parylak, K.; Zięba, Z.; Bułdys, A.; Witek, K. The verification of determining a permeability coefficient of non-cohesive soil based on empirical formulas including its microstructure. *Acta Sci. Pol.* **2013**, *12*, 43–51.
36. Salarashayeri, A.F.; Siosemarde, M. Prediction of Soil Hydraulic Conductivity from Particle Size Distribution Analysis. *World Acad. Sci. Eng. Technol.* **2012**, *6*, 16–20.
37. Twardowski, K.; Drożdżak, R. Indirect methods of estimating hydraulic properties of grounds. *Wiert. Naft. Gaz* **2006**, *23*, 477–486.
38. Bilardi, S.; Ielo, D.; Moraci, N. Predicting the Saturated Hydraulic Conductivity of Clayey Soil sand Clayey or Silty Sands. *Geosciences* **2020**, *10*, 393. [[CrossRef](#)]
39. Chapuis, R.P. Predicting the saturated hydraulic conductivity of soils: A review Bulletin of Engineering Geology and the Environment. *Bull. Eng. Geol. Environ.* **2012**, *71*, 401–434. [[CrossRef](#)]
40. Mbonimpa, M.; Aubertin, M.; Chapuis, R.P.; Bussière, B. Practical pedotransfer functions for estimating the saturated hydraulic conductivity. *Geotech. Geol. Eng.* **2002**, *20*, 235–259. [[CrossRef](#)]
41. Nash, J.E.; Sutcliffe, J.V. River flow forecasting through conceptual models. Part I. A Discussion of Principles. *J. Hydrol.* **1970**, *10*, 282–290. [[CrossRef](#)]
42. Patil, N.G.; Singh, S.K. Pedotransfer functions for estimating soil hydraulic properties: A review. *Pedosphere* **2016**, *26*, 417–430. [[CrossRef](#)]
43. Sarangi, A.; Bhattacharya, A.K. Comparison of artificial neural network and regression models for sediment loss prediction from Banha watershed in India. *Agric. Water Manag.* **2005**, *78*, 195–208. [[CrossRef](#)]
44. Sobieraj, J.A.; Elsenbeer, H.; Vertessy, R.A. Pedotransfer functions for estimating saturated hydraulic conductivity: Implications for modeling storm flow generation. *J. Hydrol.* **2001**, *251*, 202–220. [[CrossRef](#)]
45. Tiwari, A.K.; Risse, L.M.; Nearing, M.A. Evaluation of WEPP and its comparison with USLE and RUSLE. *Trans. ASAE* **2000**, *43*, 1129–1135. [[CrossRef](#)]
46. Bouma, J. Using soil survey data for quantitative land evaluation. In *Advances in Soil Science*; Stewart, B.A., Ed.; Springer: Berlin/Heidelberg, Germany, 1989; Volume 9, pp. 177–213.
47. Van Looy, K.; Bouma, J.; Herbst, M.; Koestel, J.; Minasny, B.; Mishra, U.; Montzka, C.; Nemes, A.; Pachepsky, Y.A.; Padarian, J.; et al. Pedotransfer functions in Earth system science: Challenges and perspectives. *Rev. Geophys.* **2017**, *55*, 1199–1256.

48. Briggs, L.J.; Lane, J.W.M. The moisture equivalents of soils. U.S. In *Department of Agriculture Bureau of Soils. Bulletin*; U.S. Government Printing Office: Washington, DC, USA, 1907; p. 23.
49. Cosby, B.J.; Hornberger, G.M.; Clapp, R.B.; Ginn, T.R. A statistical exploration of the relationships of soil moisture characteristic to the physical properties of soils. *Water Resour. Res.* **1984**, *20*, 682–690. [[CrossRef](#)]
50. Rawls, W.J.; Brakensiek, D.L.; Soni, B. Agricultural management effects on soil water processes. *Part I: Soil water retention and Green and Ampt infiltration parameters. Trans. ASAE* **1983**, *26*, 1747–1752.
51. Saxton, K.E.; Rawls, W.J. Soil water characteristic estimates by texture and organic matter for hydrologic solutions. *Soil Sci. Soc. Am. J.* **2006**, *70*, 1569–1578.
52. De Lannoy, G.J.M.; Koster, R.D.; Reichle, R.H.; Mahanama, S.P.P.; Liu, Q. An updated treatment of soil texture and associated hydraulic properties in a global land modeling system. *J. Adv. Model. Earth Syst.* **2014**, *6*, 957–979.
53. Ditzler, C.; Scheffe, K.; Monger, H.C.; Soil Science Division Staff. *Soil Survey Manual*; USDA Handbook No. 18; USDA: Washington DC, USA, 2017; 603p.
54. Rawles, W.; Brakensiek, D. Estimating soil water retention from soil properties. *J. Irrig. Drain. Div.* **1982**, *108*, 166–171. [[CrossRef](#)]
55. Wösten, J.H.M.; Lilly, A.; Nemes, A.; LeBas, C. Development and use of a database of hydraulic properties of European soils. *Geoderma* **1999**, *90*, 169–185.
56. Pisarczyk, S. *Elementy Budownictwa Ochrony Środowiska*; Wydawnictwo Oficyna Wydawnicza Politechniki Warszawskiej: Warszawa, Poland, 2008; p. 185.
57. Vukovic, M.; Soro, A. *Determination of Hydraulic Conductivity of Porous Media from Grain Size Composition*; Water Resources Publications: Littleton, CO, USA, 1992.
58. Saxton, K.E.; Rawls, W.J.; Romberger, J.S.; Papendick, R.I. Estimating Generalized Soil-Water Characteristics from Texture. *Soil Sci. Soc. Am. J.* **1986**, *50*, 1031–1035. [[CrossRef](#)]
59. Pazdro, Z.; Kozerski, B. *Hydrologia Ogólna*; Wydawnictwo Geologiczne: Warszawa, Poland, 1990.
60. Kozerski, B. Zasady obliczeń hydraulicznych ujęć wód podziemnych. In *Wytyczne Określenia Współczynnika Filtracji Metodami Pośrednimi i Laboratoryjnymi*; Wydawnictwo Geologiczne: Warszawa, Poland, 1977.
61. Sezer, A.; Göktepe, A.B.; Altun, S.; Bassiliades, N. Estimation of the permeability of granular soils using neuro-fuzzy system. In *Proceedings of the Workshops of the 5th IFIP Conference on Artificial Intelligence Applications & Innovations (AIAI-2009)*, Thessaloniki, Greece, 23–25 April 2009.
62. Myślińska, E. *Laboratoryjne Badania Gruntów*; Wydawnictwo Naukowe: PWN Warszawa, Poland, 1998.
63. Wösten, J.H.M.; Finke, P.A.; Jansen, M.J.W. Comparison of class and continuous pedotransfer functions to generate soil hydraulic characteristics. *Geoderma* **1995**, *66*, 227–237. [[CrossRef](#)]
64. Ryczek, M.; Kruk, E.; Malec, M.; Klatka, S. Comparison of pedotransfer functions for the determination of saturated hydraulic conductivity coefficient. *Ochr. Sr. I Zasobów Nat. Environ. Prot. Nat. Resour.* **2017**, *28*, 25–30.
65. Vereecken, H.; Maes, J.; Feyen, J.; Darius, P. Estimating the soil moisture retention characteristic from texture, bulk density, and carbon content. *Soil Sci.* **1989**, *148*, 389–403.
66. Kruk, E.; Malec, M.; Klatka, S.; Brodzińska-Cygan, A.; Kołodziej, J. Pedotransfer function for determining saturated hydraulic conductivity using artificial neural network (ANN). *Acta Sci. Pol. Form. Circumiectus* **2017**, *16*, 115–126. [[CrossRef](#)]
67. Rahnama, M.B.; Barani, G.A. Application of rainfall-runoff models to Zard river catchments. *Am. J. Environ. Sci.* **2005**, *1*, 86–89.
68. Kondracki, J. *Geografia Regionalna Polski*; Wydawnictwo Naukowe PWN: Warszawa, Poland, 2000.
69. Weynants, M.; Vereecken, H.; Javaux, M. Revisiting Vereecken pedotransfer functions: Introducing a closed-form hydraulic model. *Vadose Zone* **2009**, *81*, 86.

Disclaimer/Publisher’s Note: The statements, opinions and data contained in all publications are solely those of the individual author(s) and contributor(s) and not of MDPI and/or the editor(s). MDPI and/or the editor(s) disclaim responsibility for any injury to people or property resulting from any ideas, methods, instructions or products referred to in the content.